Perturbative Particle Simulation Studies of Periodically Focused Intense Charged Particle Beams. [1]

Weihua Zhou, Hong Qin and Ronald C. Davidson
Plasma Physics Laboratory, Princeton University
Princeton, NJ 08543, USA

June 12, 2007

[1] Research supported by the U.S. Department of Energy

Abstract

High intensity charged particle beam propagation in a periodic focusing lattice has been studied numerically using a model in which the beam equilibrium and dynamic behavior are described self-consistently by the nonlinear Vlasov-Maxwell equations. For a long coasting which is inhomogeneous in the transverse direction, the solutions to the Vlasov-Maxwell equations for periodic focusing configurations can only be determined numerically. To carry out this investigation, the Beam Equilibrium Stability and Transport (BEST) code which uses a 3D low-noise perturbative particle simulation method, has been extended. The scheme begins with a smooth-focusing lattice which is the smooth-focusing approximation for the periodic lattice, and adiabatically replaces the smooth-focusing lattice by the periodic lattice. With this approach, periodic solenoidal configurations have been investigated using a slow turn-on time to minimize beam mismatch, and periodic quadrupole configurations are now being studied.

Objective and Method

- The objective is to find practical solutions for Intense Charged Particle Beam (ICPB) in Periodic Focusing Configurations so that we can determine the detailed equilibrium, stability, and transport properties;
- BEST code is used to numerically solve the Vlasov-Maxwell equations;
- With the δf simulation method, the BEST code succeeds in reducing the noise by a factor of $\frac{f}{\delta f}$;
- To apply the δf simulation method, the numerical scheme begins with a smooth-focusing lattice model for the periodic lattice, and adiabatically replaces the smooth-focusing lattice by the periodic lattice.

Current Status of the Problem

- Analytical approch:
  - The nonlinearity of the Vlasov-Maxwell equations makes it impossible to find a general analytical solution;
  - The only analytical solution is the Kapchinskij-Vladimirskij distribution, which is of limited practical interest;
  - Using Hamiltonian Averaging Techniques, it is possible to obtain approximate analytical solutions.
- Numerically, the δf simulation method is promising. To apply this method, a "quasi-equilibrium" solution is needed.

Vlasov-Maxwell Equations

The Vlasov-Maxwell equations in a two-dimensional slice model are:

$$\left\{ \frac{\partial}{\partial s} + x' \frac{\partial}{\partial x} + y' \frac{\partial}{\partial y} - \left(\kappa_x(s)\, x + \frac{\partial \psi}{\partial x} \right) \frac{\partial}{\partial x'} - \left(\kappa_y(s)\, y + \frac{\partial \psi}{\partial y} \right) \frac{\partial}{\partial y'} \right\} F_b = 0,$$

and

$$\left(\frac{\partial^2}{\partial x^2} + \frac{\partial^2}{\partial y^2} \right) \psi = -\frac{2\pi K_b}{N_b} \int dx'\, dy'\, F_b,$$

in which $\kappa_x(s)$ and $\kappa_y(s)$ are lattice functions, and the transverse focusing force on a beam particle is given by $\mathbf{F}_{foc} = -\left[\kappa_x(s)\, x \hat{\mathbf{e}}_x + \kappa_y(s)\, y \hat{\mathbf{e}}_y\right]$.

Here, $K_b = 2N_b e_b^2 / \gamma_b^3 m_b \beta_b^2 c^2$ is the self-field perveance, and $\psi = e_b \phi / \gamma_b^3 m_b \beta_b^2 c^2$ is the normalized self-field potential.

Periodic Focusing Solenoidal Field

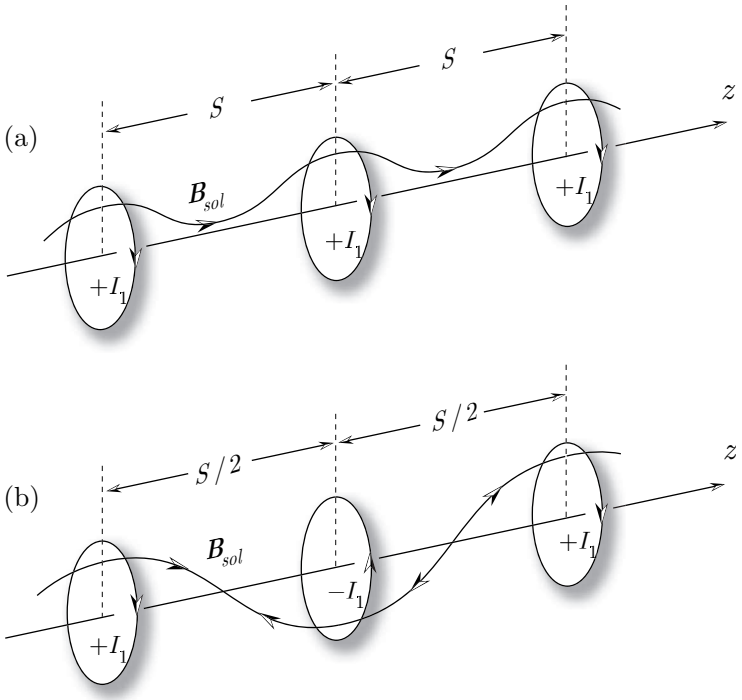

Figure: Periodic Focusing Solenoidal field

- The magnetic field is given by:

$$\mathbf{B}_{sol}(\mathbf{x}) = -\frac{1}{2}B_z'(z)(x\hat{\mathbf{e}}_x + y\hat{\mathbf{e}}_y) + B_z(z)\,\hat{\mathbf{e}}_z$$

$$\mathbf{A}_{sol}(\mathbf{x}) = \frac{1}{2}B_z(z)(x\hat{\mathbf{e}}_y - y\hat{\mathbf{e}}_x) = \frac{1}{2}B_z(z)\,r\hat{\mathbf{e}}_\theta$$

- Periodic variation:

$$B_z(z+S) = B_z(z)$$

- The lattice functions are given by:

$$\kappa_x(s) = \kappa_y(s) \equiv \kappa_z(s) = \left(\frac{e_b B_z(z)}{2\gamma_b m_b \beta_b c^2}\right)^2$$

- In general,

$$\int_{s_0}^{s_0+S} ds\,\kappa_z(s) \neq 0$$

Alternating-gradient Quadrupole Field

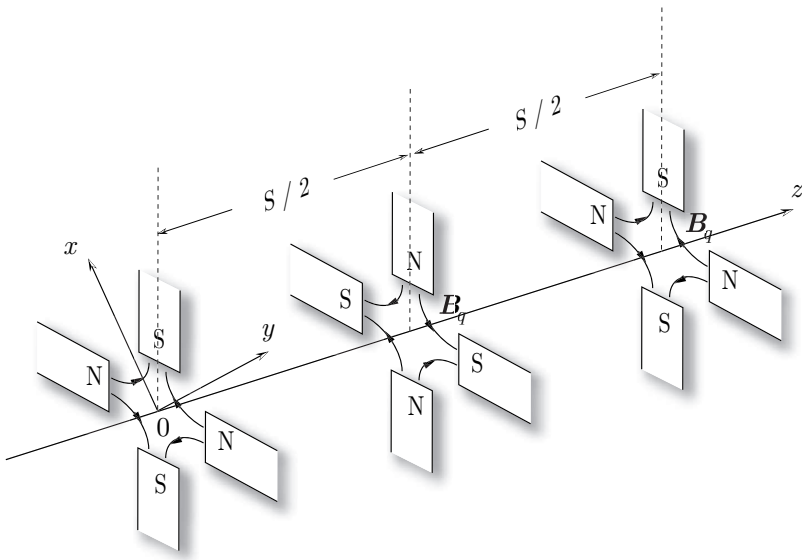

Figure: An alternating-gradient quadrupole field

- The magnetic field is given by:

$$\mathbf{B}_q(\mathbf{x}) = B_q'(z)\left(y\hat{\mathbf{e}}_x + x\hat{\mathbf{e}}_y\right),$$
$$\mathbf{A}_q(\mathbf{x}) = -\frac{1}{2}B_q'(z)\left(x^2 - y^2\right)\hat{\mathbf{e}}_z.$$

- Periodic variation:

$$B_q'(z+S) = B_q'(z)$$

- The lattice functions are given by:

$$\kappa_x(s) = -\kappa_y(s) \equiv \kappa_q(s) = \frac{e_b B_q'(s)}{\gamma_b m_b \beta_b c^2}$$

- $\kappa_q(s)$ satisfies:

$$\int_{s_0}^{s_0+S} ds\, \kappa_q(s) = 0$$

Simulation Scheme I

- Define F_b^0 as a zeroth-order equilibrium distribution function which satisfies

$$\frac{\partial F_b^0}{\partial s} + \mathbf{X}' \cdot \frac{\partial F_b^0}{\partial \mathbf{X}} + \left(-\kappa_{sf}\mathbf{X} - \frac{\partial \psi^0}{\partial \mathbf{X}} \right) \cdot \frac{\partial F_b^0}{\partial \mathbf{X}'} = 0,$$

$$\left(\frac{\partial^2}{\partial X^2} + \frac{\partial^2}{\partial Y^2} \right) \psi^0 = -\frac{2\pi K_b}{N_b} \int dX'\, dY'\, F_b^0,$$

  κ_{sf} is obtained in the smooth-focusing approximation.

- For a solenoidal lattice,

$$\kappa_{sf} = \overline{\kappa}_z + \left[\left\langle \left(\int_{s_0}^{s} ds\, \delta\kappa_z(s) \right)^2 \right\rangle - \left\langle \left(\int_{s_0}^{s} ds\, \delta\kappa_z(s) \right) \right\rangle^2 \right]$$

  where $\overline{\kappa}_z \equiv (1/S) \int_{s_0}^{s_0+S} ds\, \kappa_z(s)$.

- For a quadrupole lattice,

$$\kappa_{sf} = \left\langle \left(\int_{s_0}^{s} ds\, \kappa_q(s) \right)^2 \right\rangle - \left\langle \left(\int_{s_0}^{s} ds\, \kappa_q(s) \right) \right\rangle^2$$

Simulation Scheme II

- Define δF_b and w as $\delta F_b \equiv F_b - F_b^0$, $w \equiv \dfrac{\delta F_b}{F_b}$. The dynamical equation for w is given by

$$\frac{d}{ds} w = (1-w) \left\{ \left(\delta\kappa_x(s) X + \frac{\partial}{\partial X} \delta\psi \right) \frac{1}{F_b^0} \frac{\partial F_b^0}{\partial X'} + \left(\delta\kappa_y(s) Y + \frac{\partial}{\partial Y} \delta\psi \right) \frac{1}{F_b^0} \frac{\partial F_b^0}{\partial Y'} \right\}$$

with $\delta\psi(X, Y, s)$ determined by

$$\left(\frac{\partial^2}{\partial X^2} + \frac{\partial^2}{\partial Y^2} \right) \delta\psi = -\frac{2\pi K_b}{N_b} \int dX'\, dY'\, w F_b = -\frac{2\pi K_b}{N_b} \int dX'\, dY'\, \frac{w}{1-w} F_b^0$$

- Here, at $s = 0$, $\delta\kappa_x(s) = \delta\kappa_y(s) = 0$;
- For s large enough,

$$\delta\kappa_x(s) = \delta\kappa_y(s) \to \kappa_z(s) - \kappa_{sf}$$

for a solenoidal lattice, and

$$\delta\kappa_x(s) \to \kappa_q(s) - \kappa_{sf}, \;\; \delta\kappa_y(s) \to -\kappa_q(s) - \kappa_{sf}$$

for a quadrupole lattice.

Turning on the Solenoidal Lattice

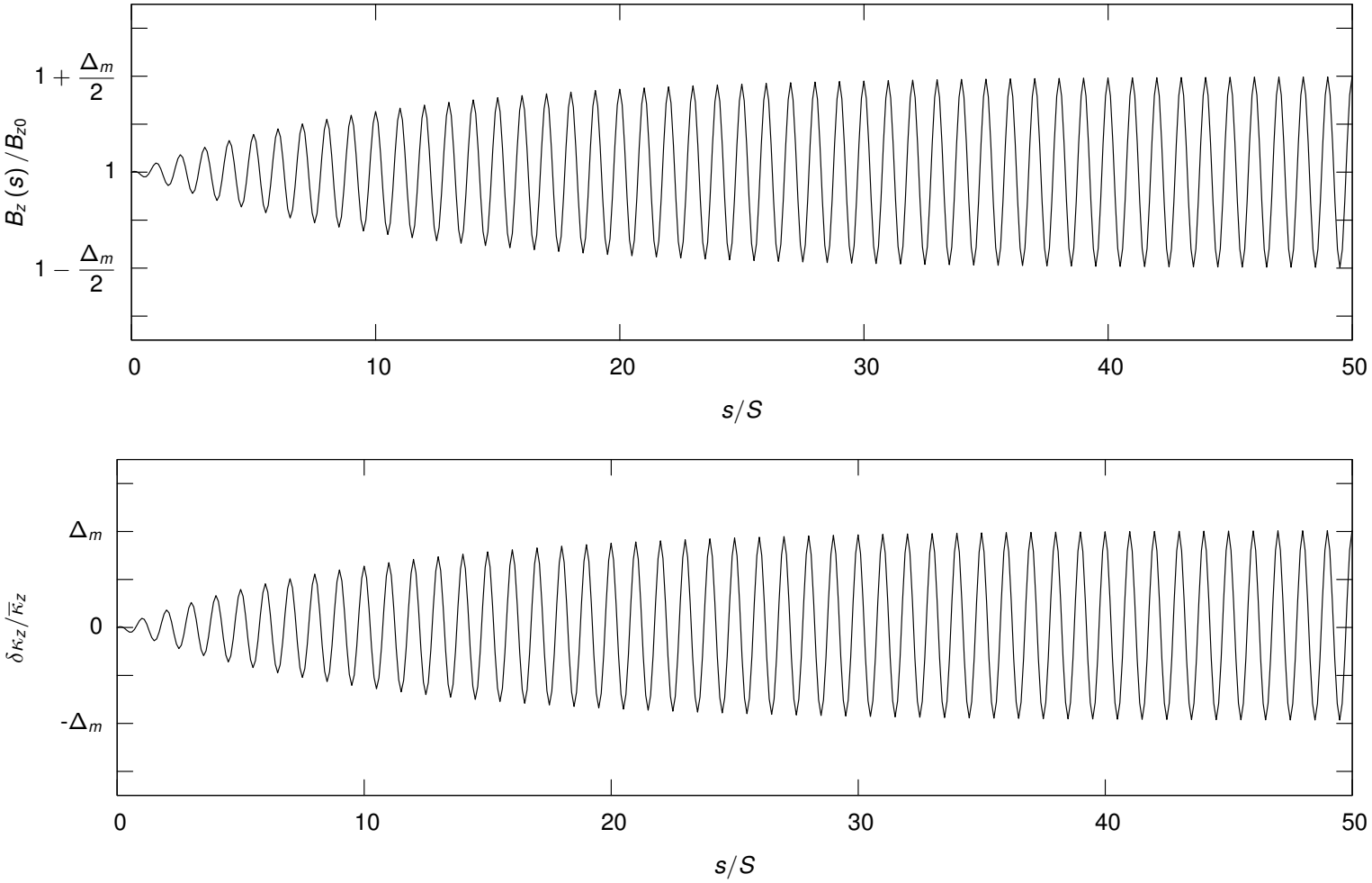

$B_z(s)$ is given by $B_z(s) = B_{z0}\left[1 + (\Delta_s/2)\cos(2\pi s/S)\right]$, where $\Delta_s = \Delta_m\left[1 - \exp(-s/NS)\right]$, and N is the number of lattice periods for turn-on. In the figure, N=10.

Adiabatic Model for the Solenoidal Lattice (I)

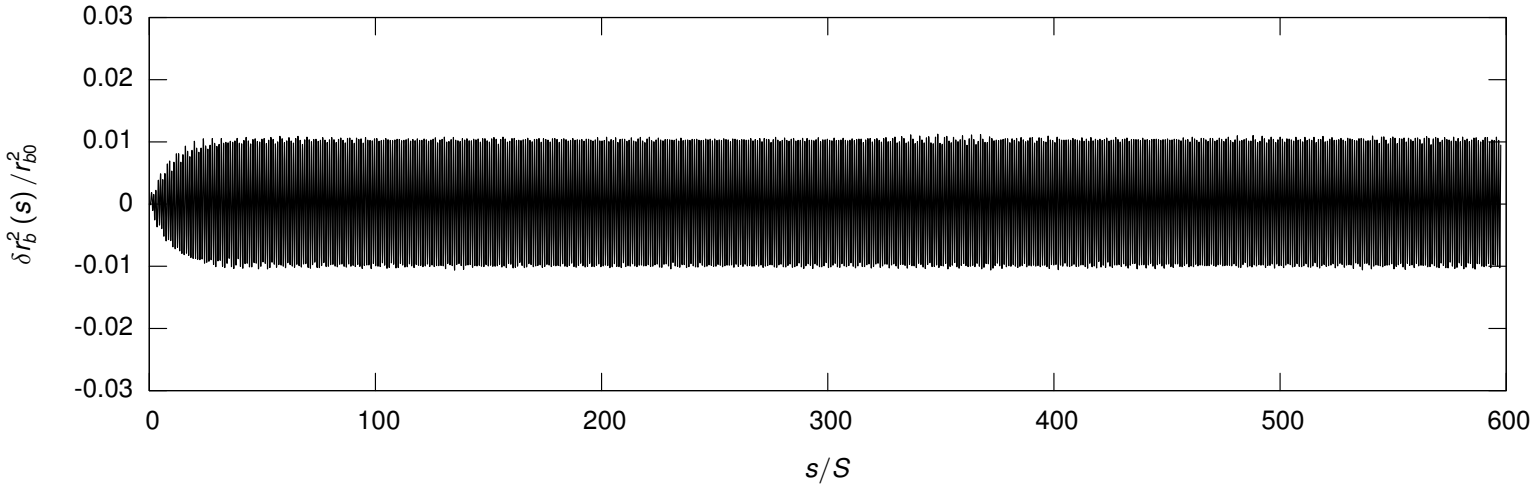

Figure: Time evolution of root mean square radius for the adiabatic model I

$$s_b = 0.2, \Delta_m = 0.2, N = 10$$

where $s_b = \omega_{pb}^2/2\gamma_b^2\omega_{\beta\perp}^2$ is the normalized beam intensity.

Adiabatic Model for the Solenoidal Lattice (I)

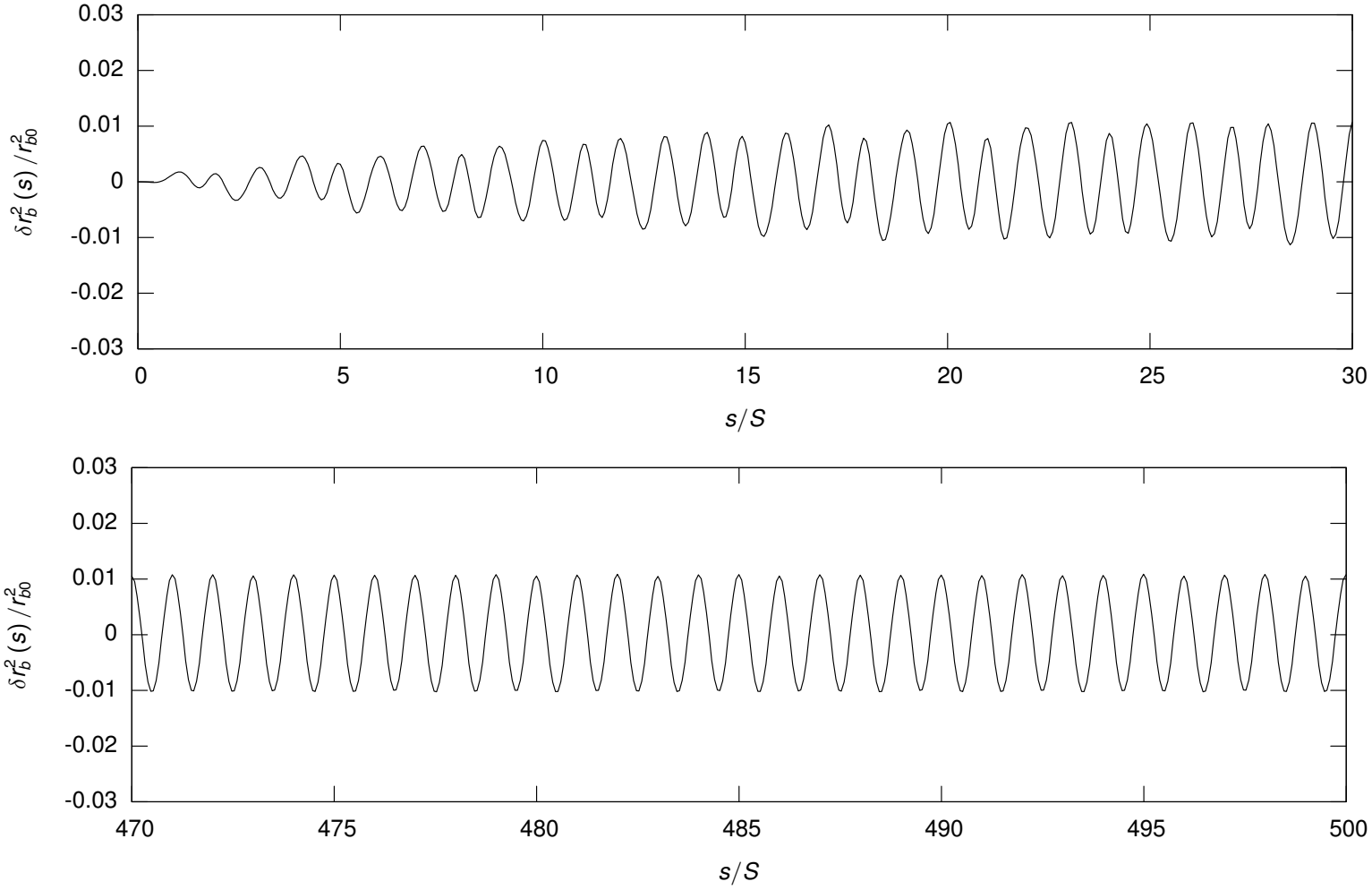

Figure: Time evolution of root mean square radius for the adiabatic model I

FFT of the Beam Radius Perturbation (I)

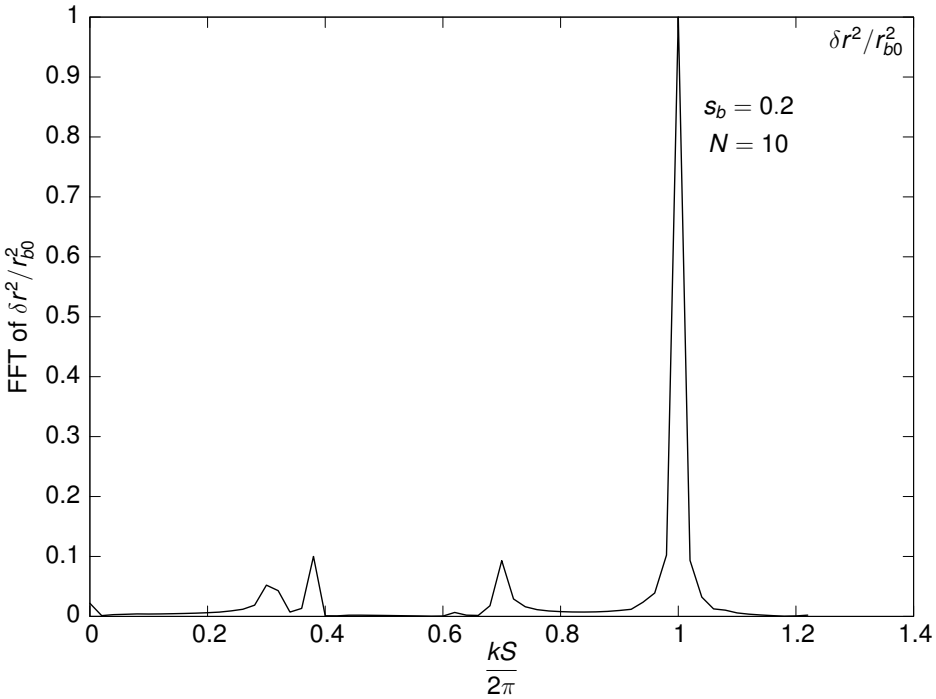

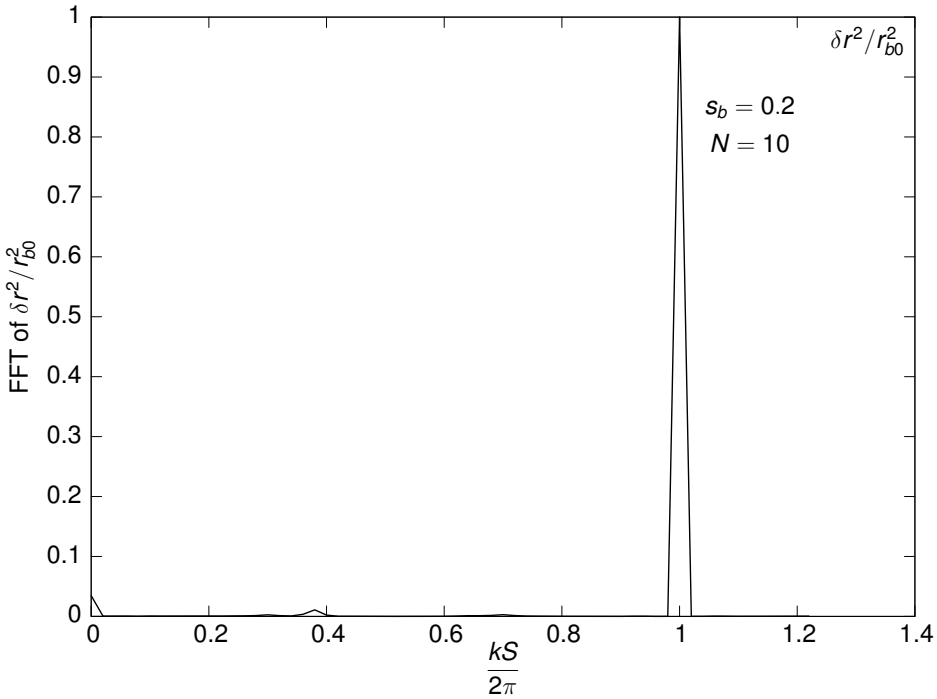

Figure: FFT of $\delta r^2(s)/r_{b0}^2$ for $N = 10$. The left figure is FFT from $s = 0$ to $s = 30S$, and the right figure is FFT from $s = 470S$ to $s = 500S$.

After sufficient time, we obtain a well-matched periodically-focused beam.

Adiabatic Model for the Solenoidal Lattice (II)

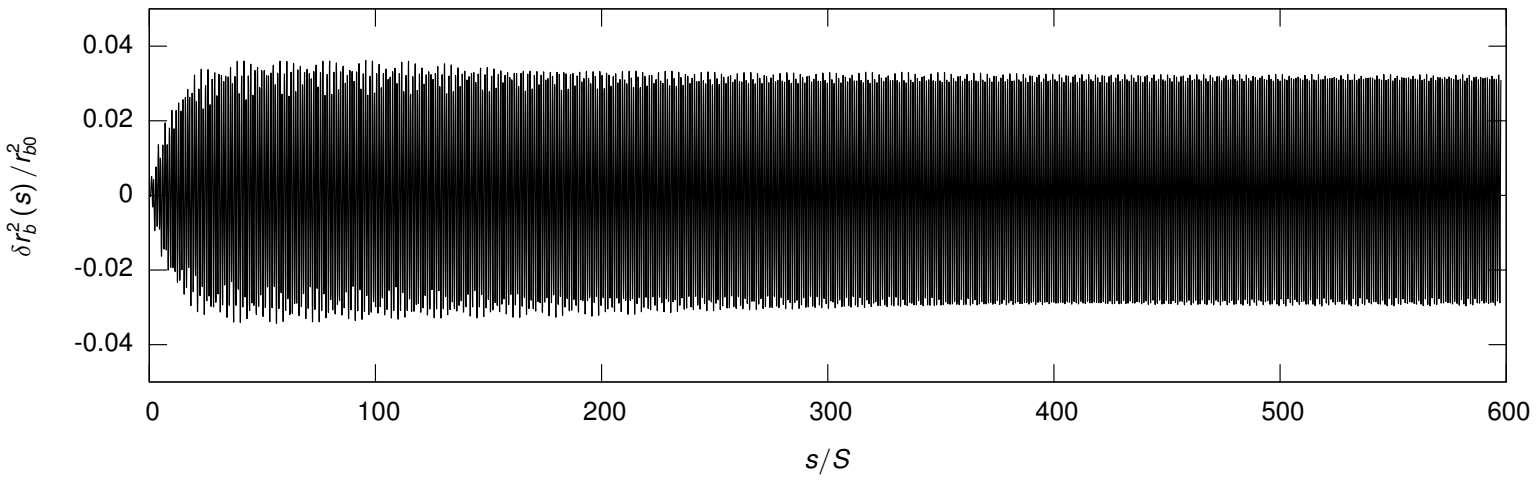

Figure: Time evolution of root mean square radius for the adiabatic model II

$$s_b = 0.2, \Delta_m = 0.6, N = 10$$

Adiabatic Model for the Solenoidal Lattice (II)

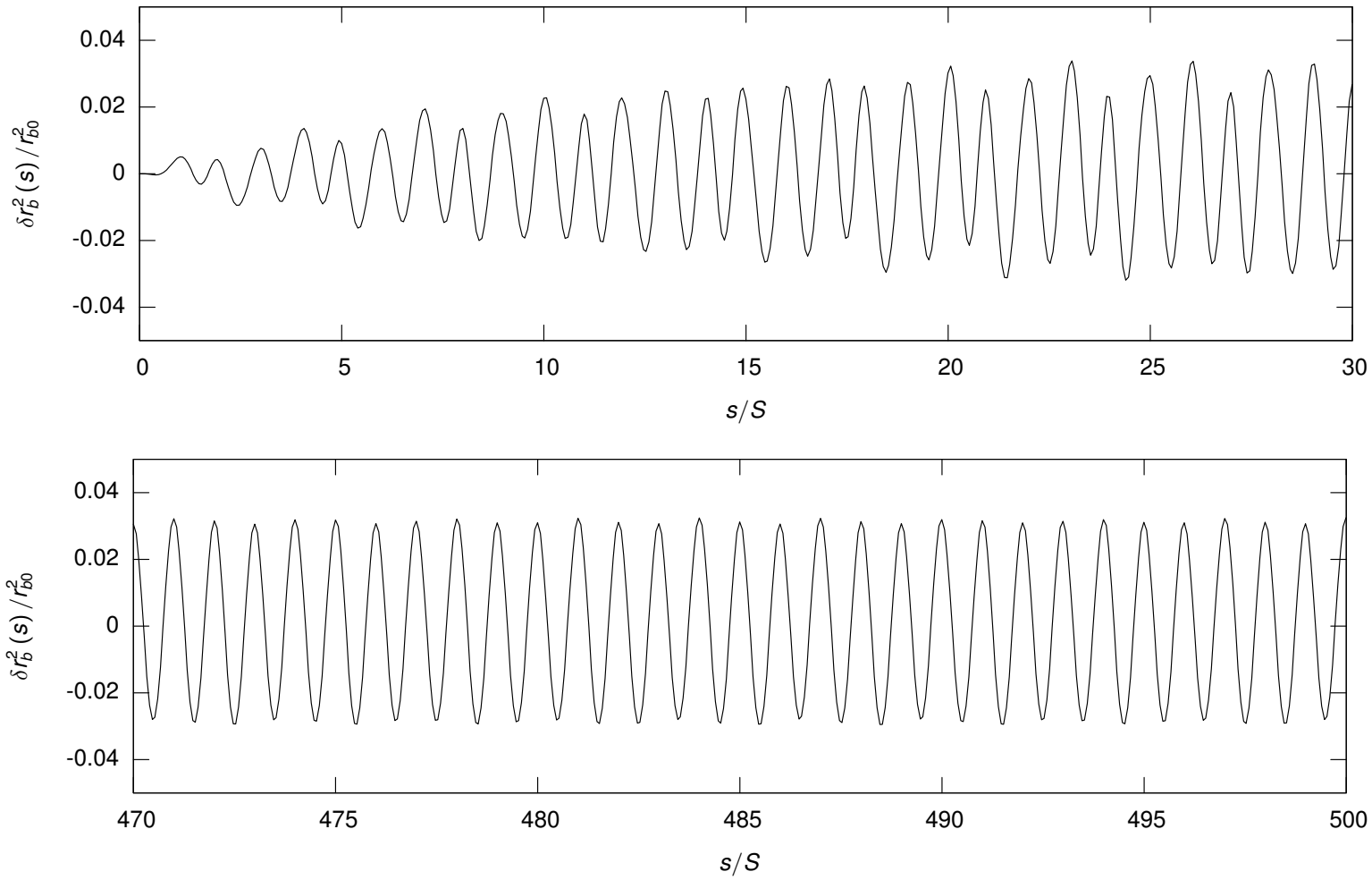

Figure: Time evolution of root mean square radius for the adiabatic model II for $\Delta_m = 0.6$

FFT of the Beam Radius Perturbation (II)

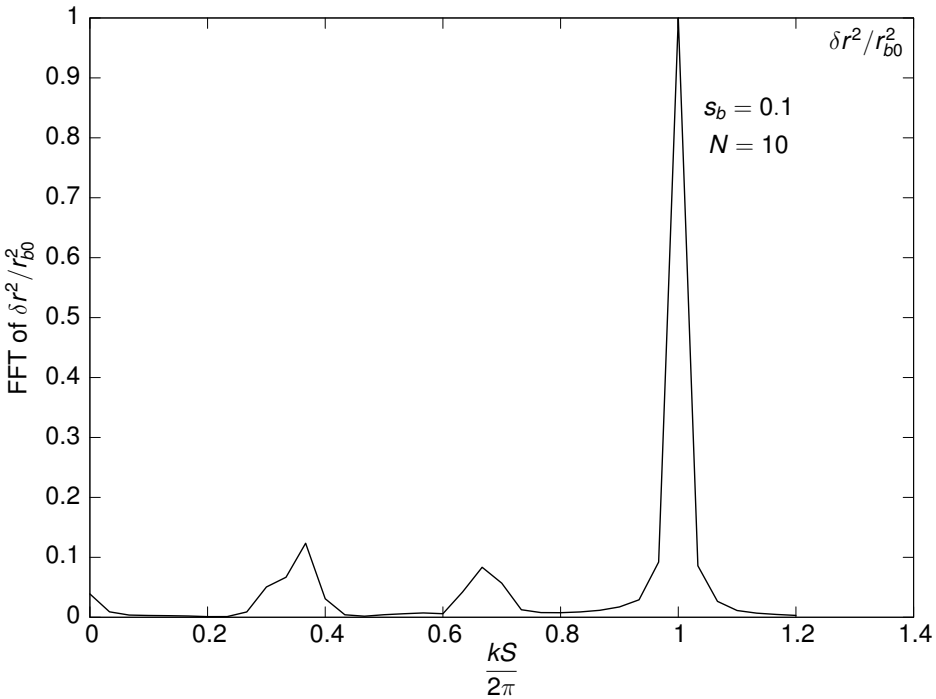

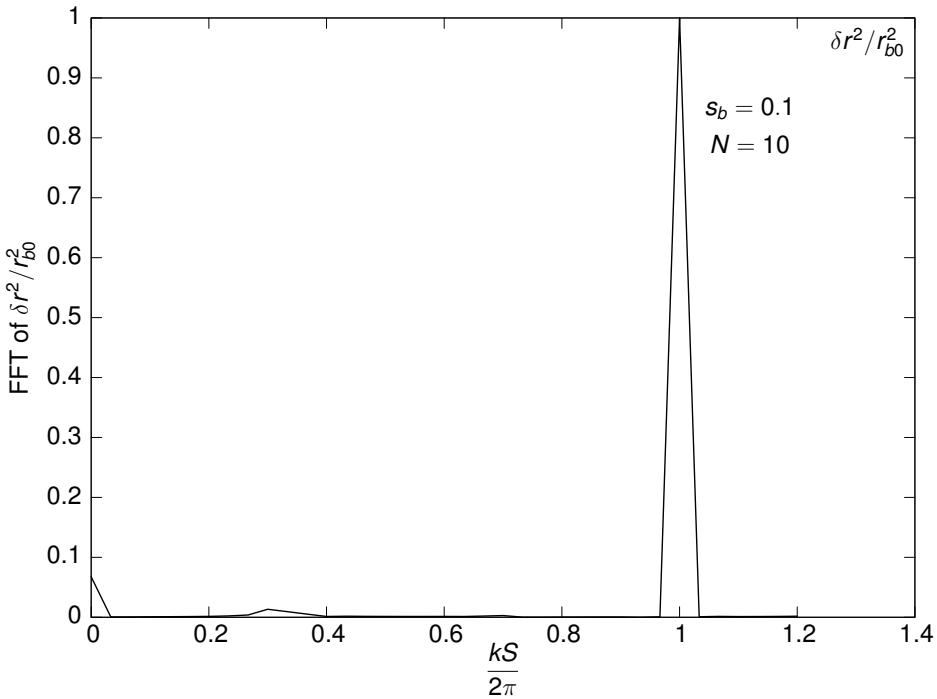

Figure: FFT of $\delta r^2(s)/r_{b0}^2$ for $N = 10$ and $\Delta_m = 0.6$. The left figure is FFT from $s = 0$ to $s = 30S$, and the right figure is FFT from $s = 470S$ to $s = 500S$.

After sufficient time, we also obtain a well-matched periodically-focused beam.

Adiabatic Model for the Solenoidal Lattice (III)

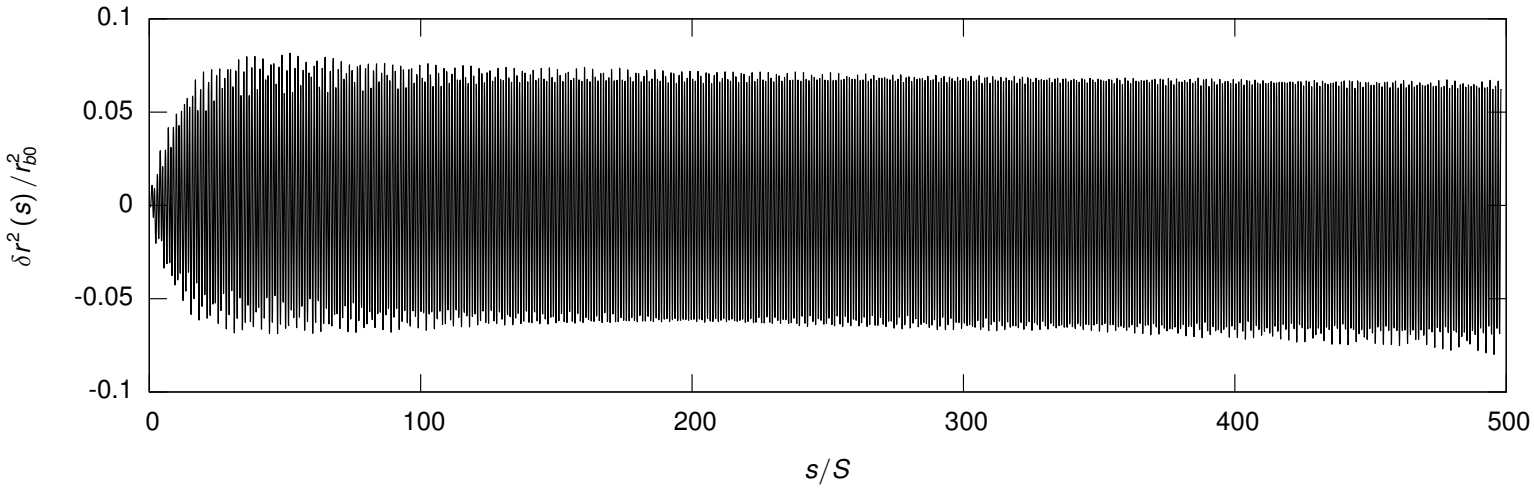

Figure: Time evolution of root mean square radius for the adiabatic model III

$$s_b = 0.2, \Delta_m = 1.8, N = 10$$

Adiabatic Model for the Solenoidal Lattice (III)

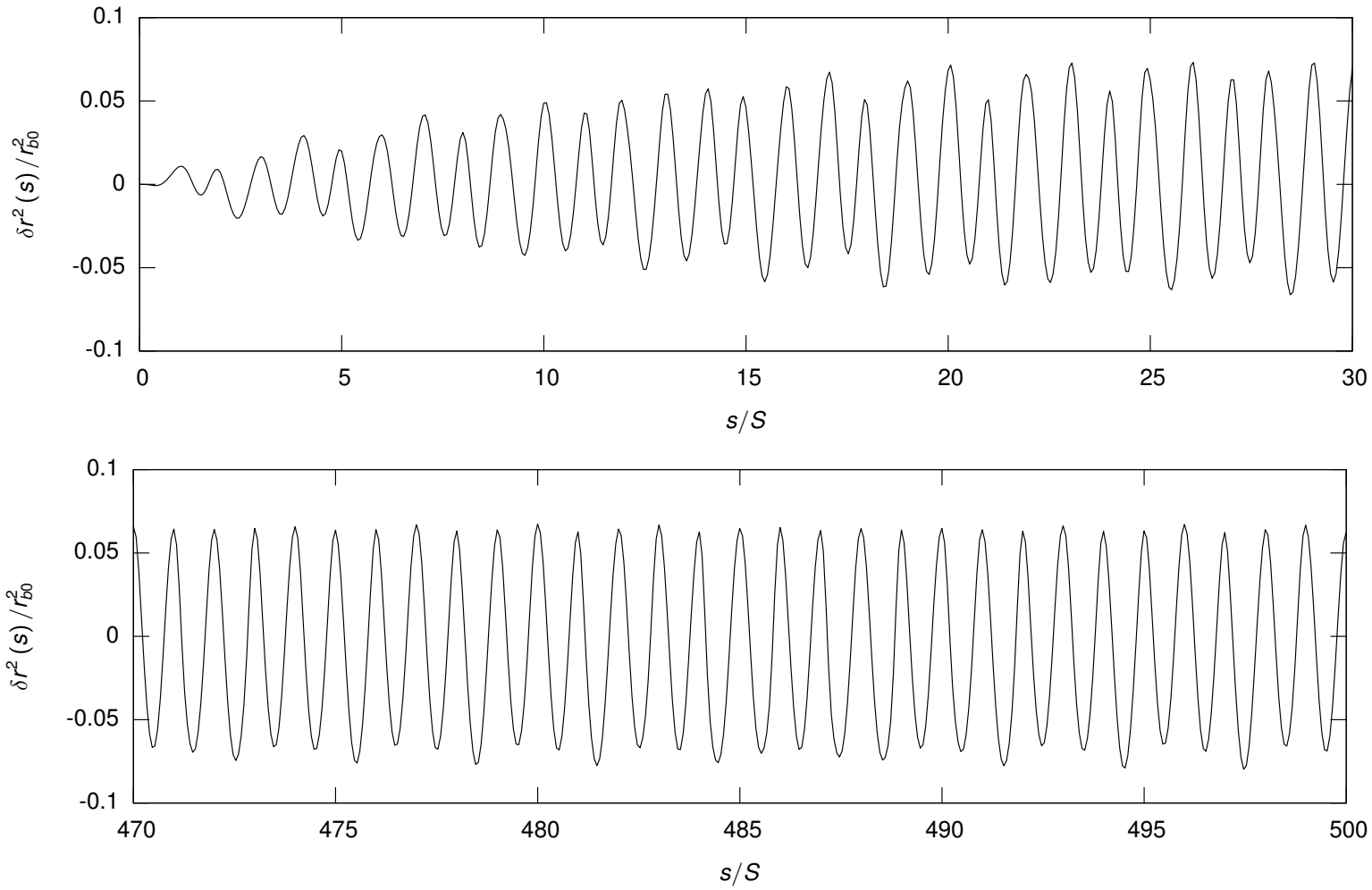

Figure: Time evolution of root mean square radius for the adiabatic model III for $\Delta_m = 1.8$

δr_b^2 for Different N

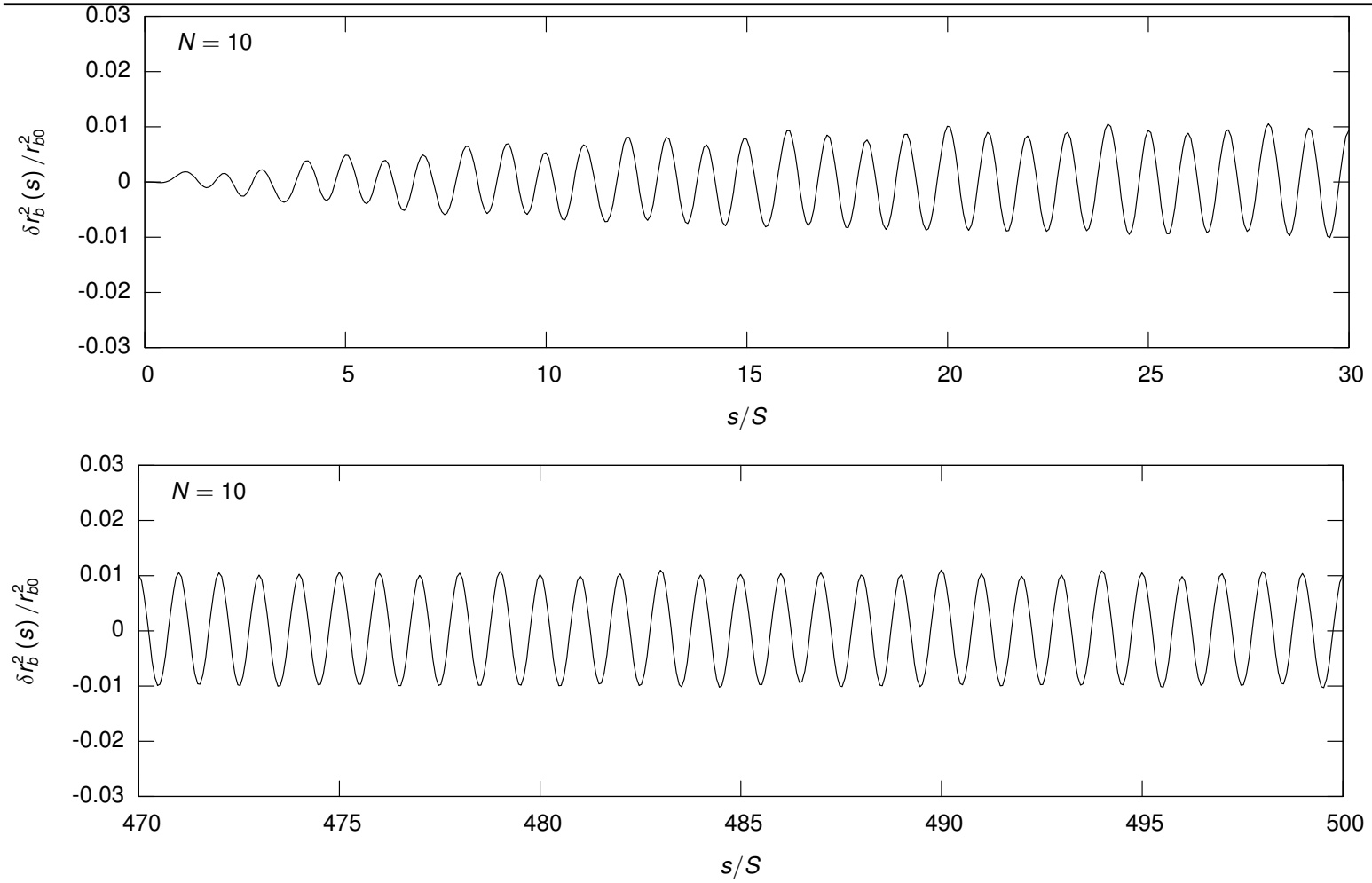

Figure: Time evolution of root mean square radius for $N = 10$ (slow turn-on)

$$s_b = 0.9, \Delta_m = 0.2$$

δr_b^2 for Different N

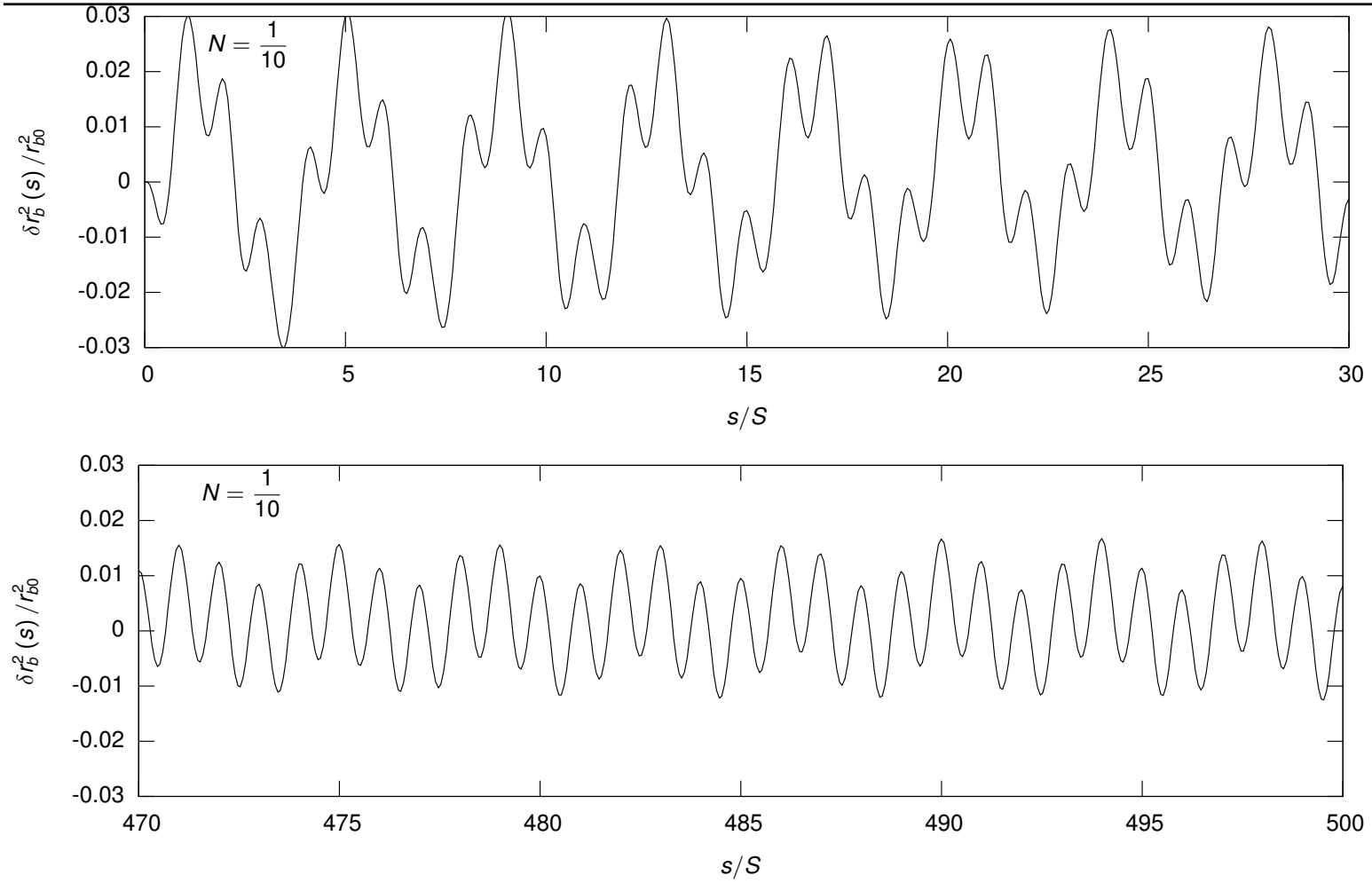

Figure: Time evolution of root mean square radius for $N = 0.1$ (fast turn-on)

$$s_b = 0.9, \Delta_m = 0.2$$

FFT of the Beam Radius Perturbation for Different N

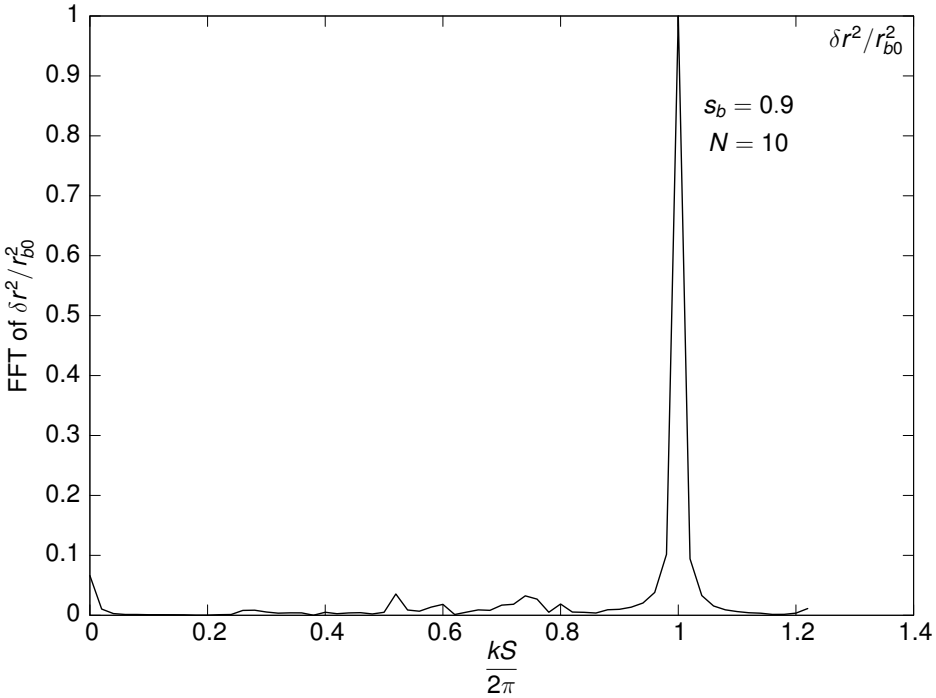

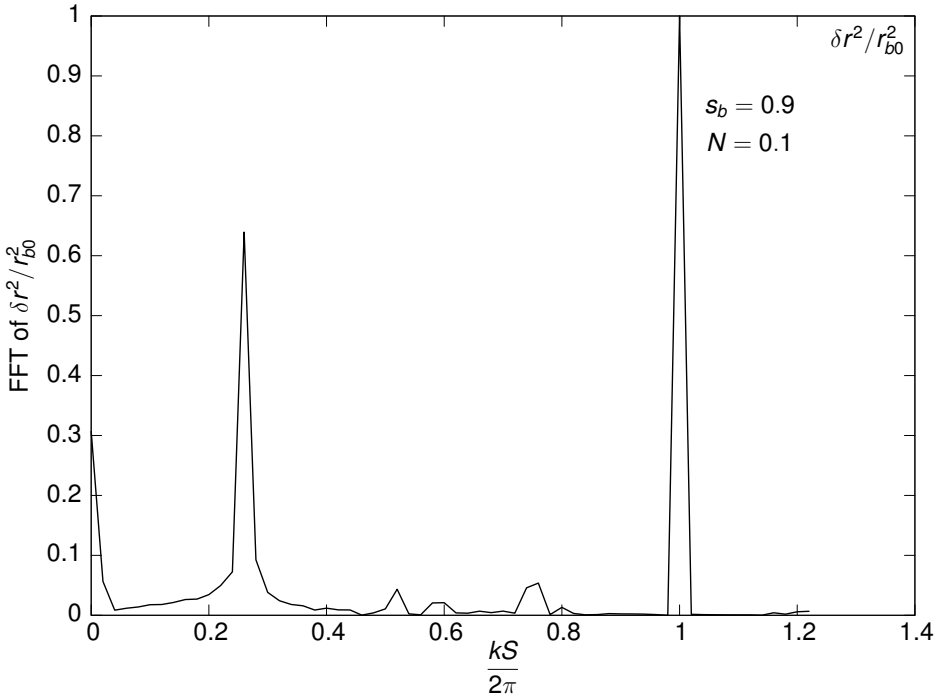

Figure: FFT of $\delta r^2(s)/r_{b0}^2$ from $s = 0$ to $s = 30S$. The left figure is for $N = 10$ (slow turn-on), and the right figure is for $N = 0.1$ (fast turn-on).

FFT of the Beam Radius Perturbation for Different N

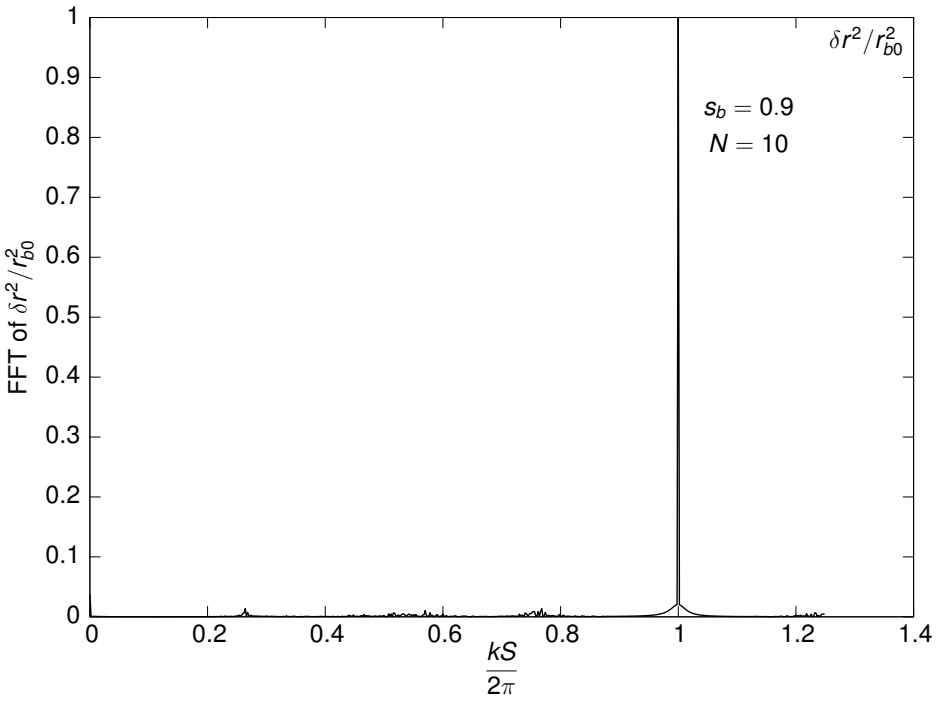

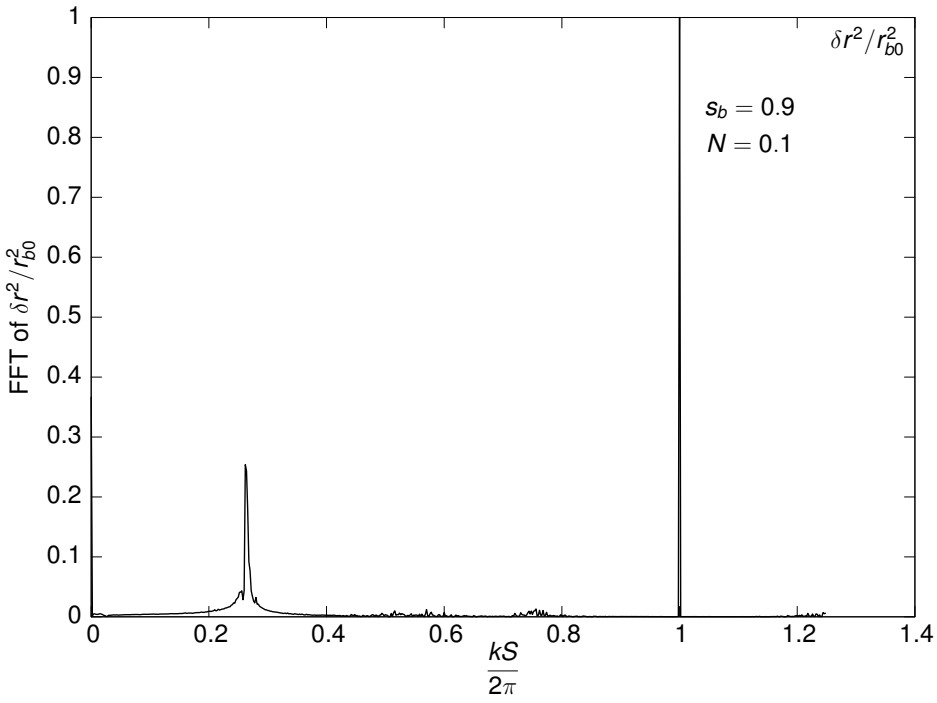

Figure: FFT of $\delta r^2(s)/r_{b0}^2$ from $s = 0$ to $s = 500S$. The left figure is for $N = 10$ (slow turn-on), and the right figure is for $N = 0.1$ (fast turn-on).

Larger $N \Rightarrow$ better beam matching.

FFT of the Beam Radius Perturbation for Different s_b

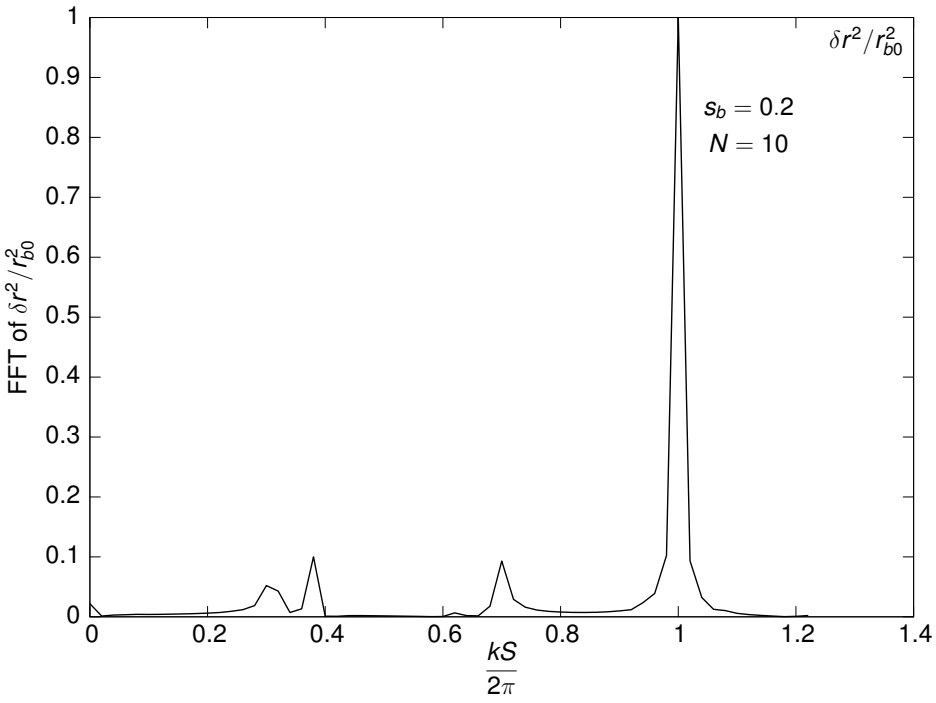

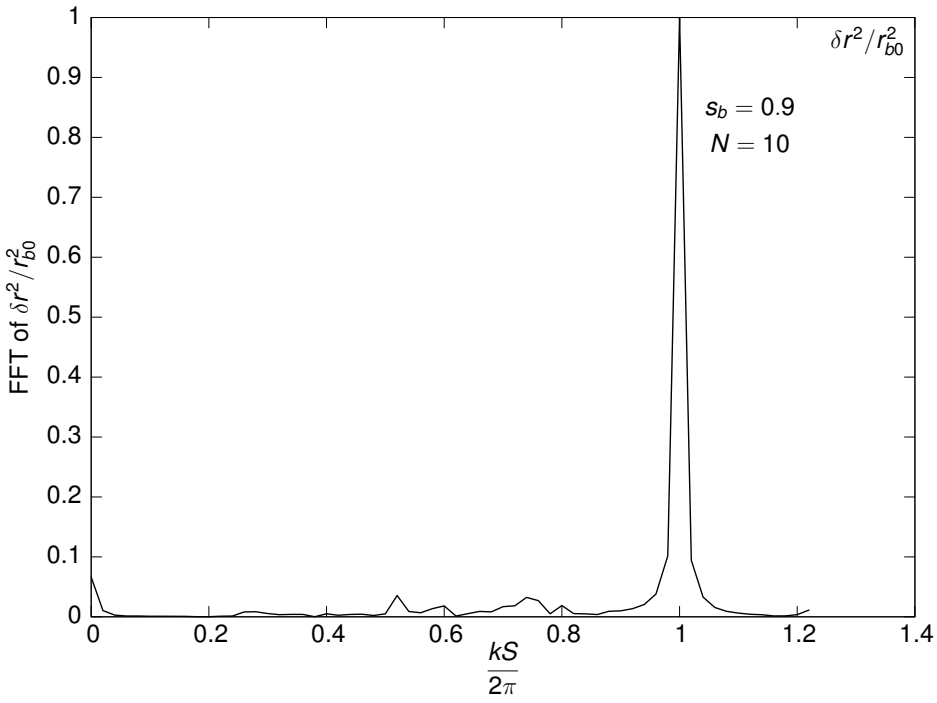

Figure: FFT of $\delta r^2(s)/r_{b0}^2$ from $s = 0$ to $s = 30S$. The left figure is for $s_b = 0.2$ and the right figure is for $s_b = 0.9$. Both are for $N = 10$ (slow turn-on).

Larger $s_b \Rightarrow$ somewhat better beam matching.

FFT of the Beam Radius Perturbation for Different s_b

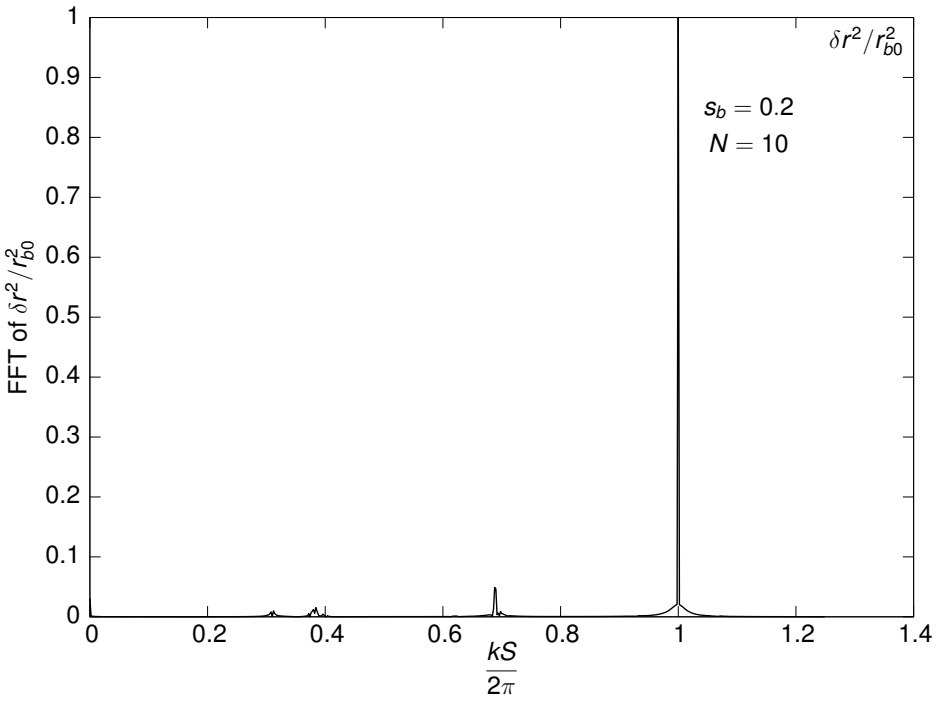

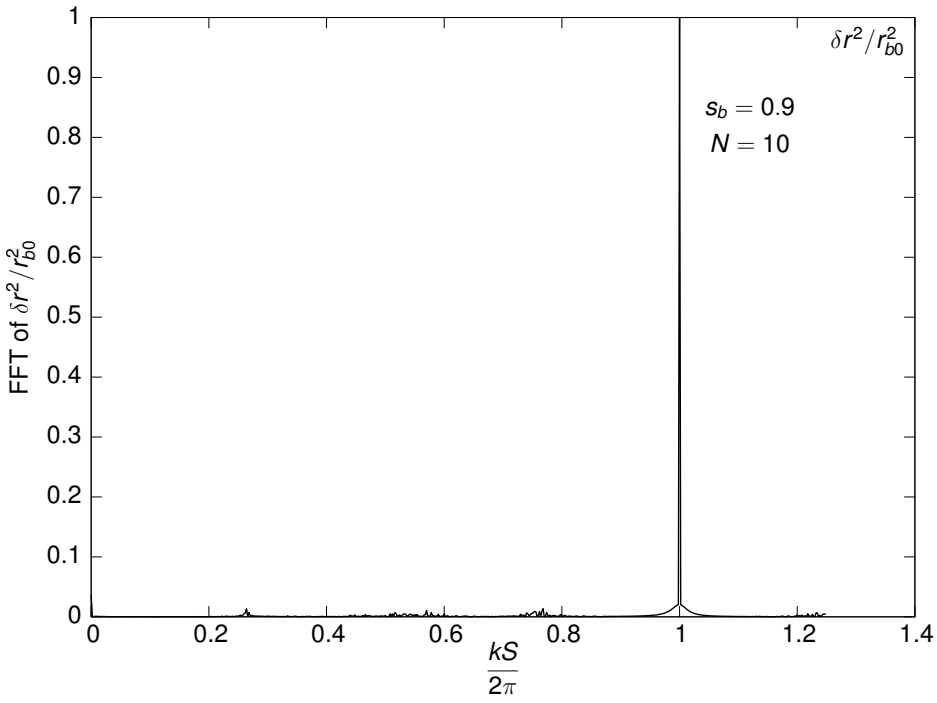

Figure: FFT of $\delta r^2(s)/r_{b0}^2$ from $s = 0$ to $s = 500S$. The left figure is for $s_b = 0.2$ and the right figure is for $s_b = 0.9$. Both are for $N = 10$ (slow turn-on).

Larger $s_b \Rightarrow$ somewhat better beam matching.

Turning on the Quadrupole Lattice

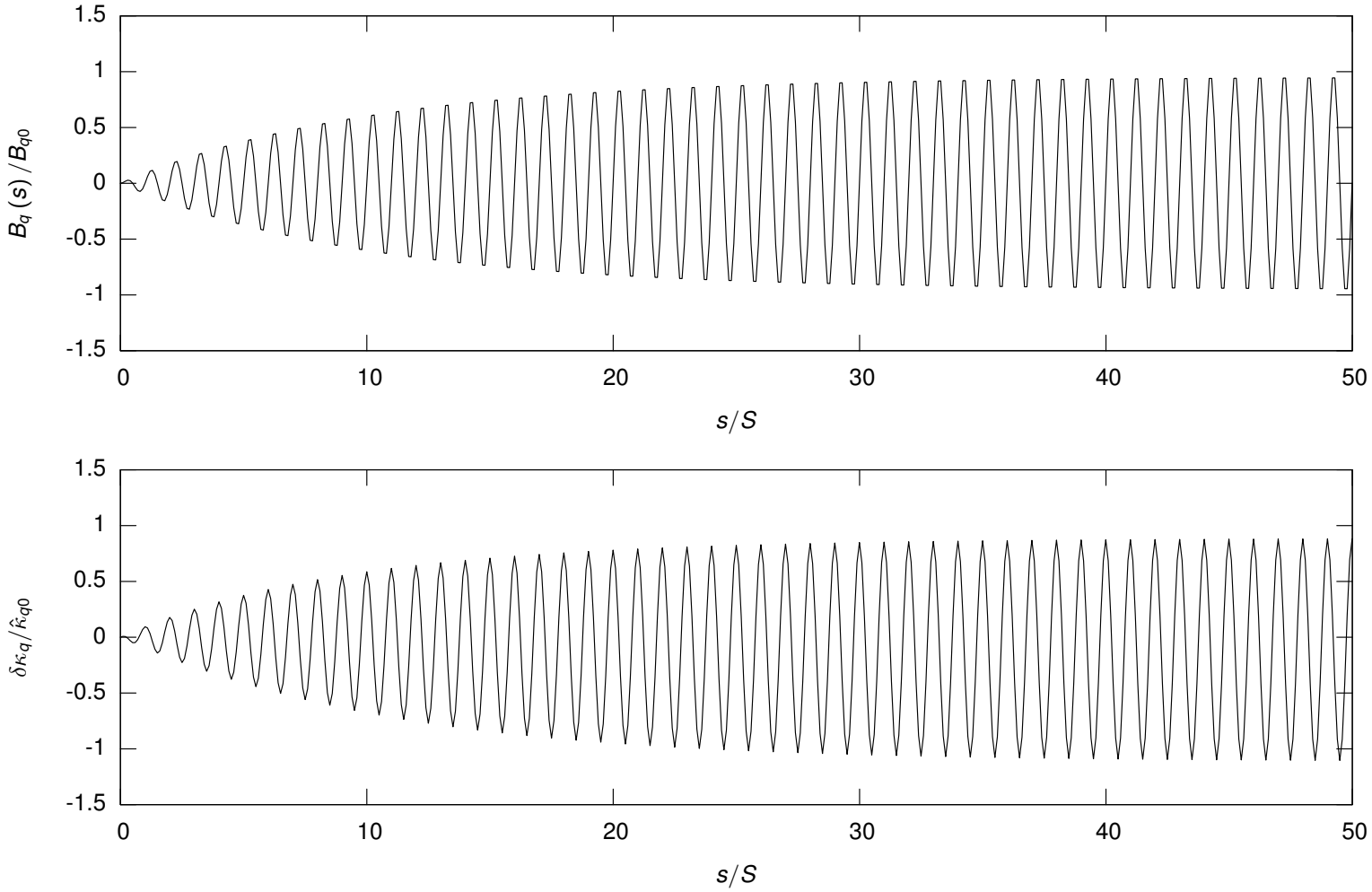

$B_q(s)$ is given by $B_q(s) = B_{q0}\Delta_s \sin(2\pi s/S)$, where $\Delta_s = [1 - \exp(-s/NS)]$, and N is the number of lattice periods for turn-on. In the figure, N=10.

Adiabatic Model for the Quadrupole Lattice

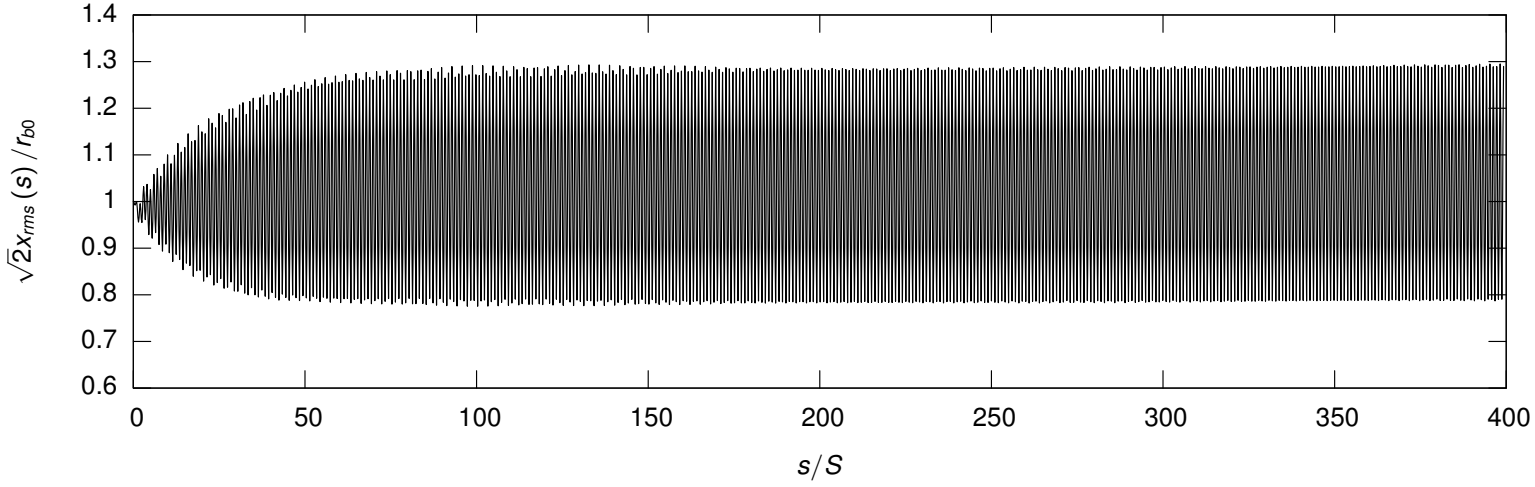

Figure: Time evolution in the **x** direction for $N = 20$ (slow turn-on). In the figure, x_{rms} is the root mean square x for all the particles.

$$s_b = 0.1, \sigma_v = 57.3^\circ$$

where σ_v is the vacuum phase advance.

Adiabatic Model for the Quadrupole Lattice

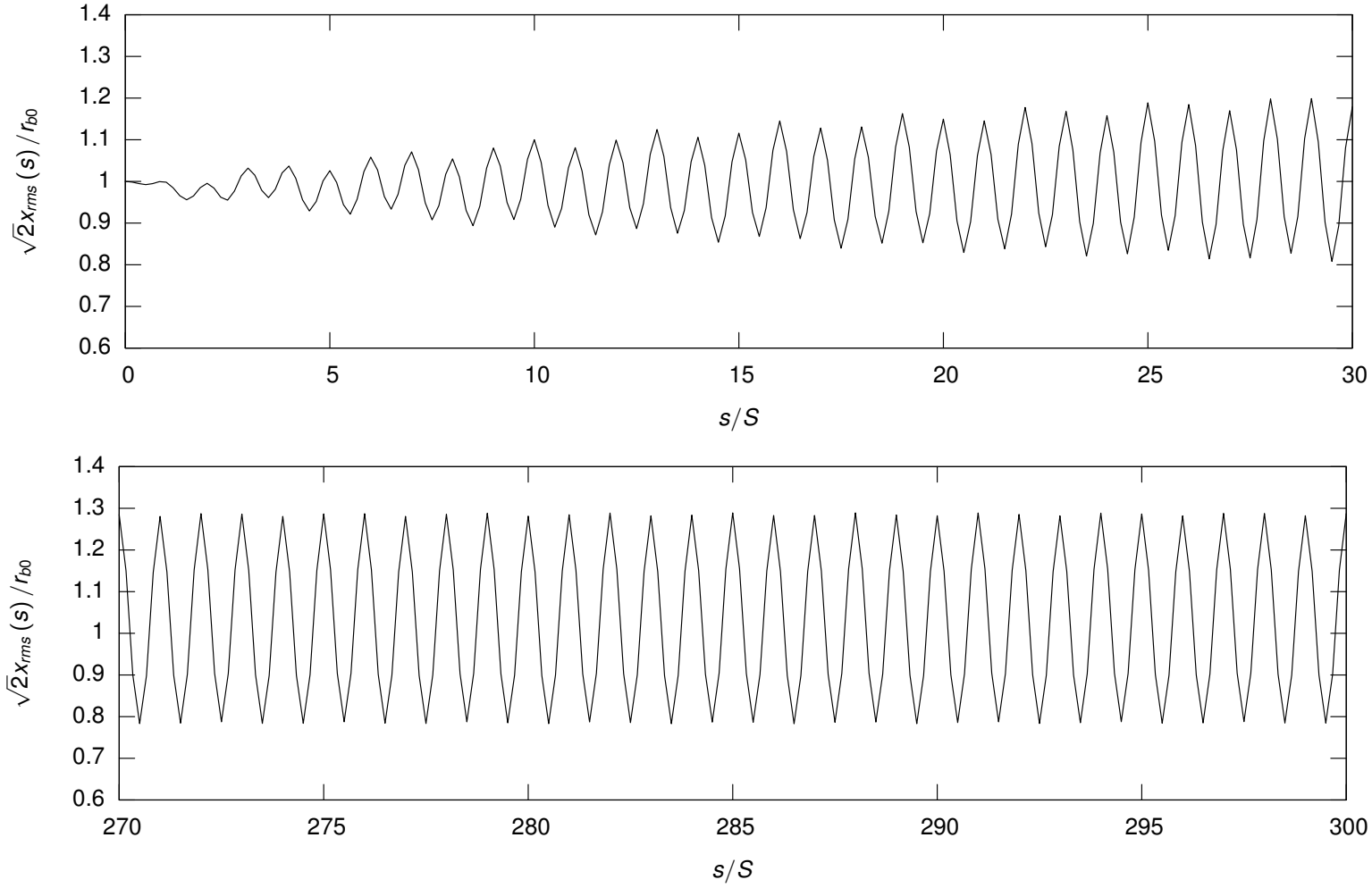

Figure: Time evolution in the **x** direction for $N = 20$ (slow turn-on)

FFT of the Root Mean Square x

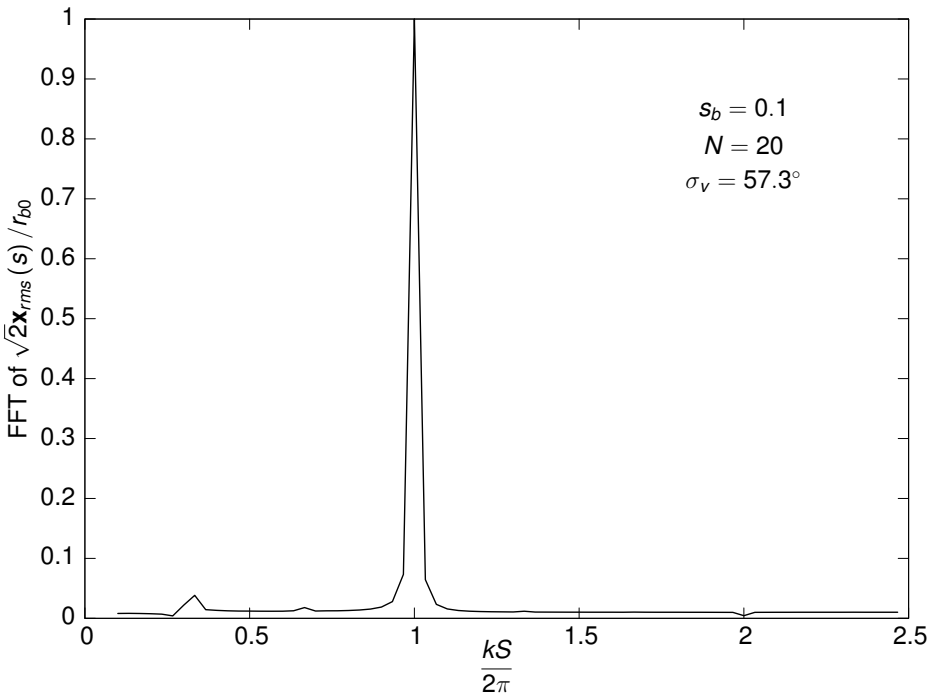

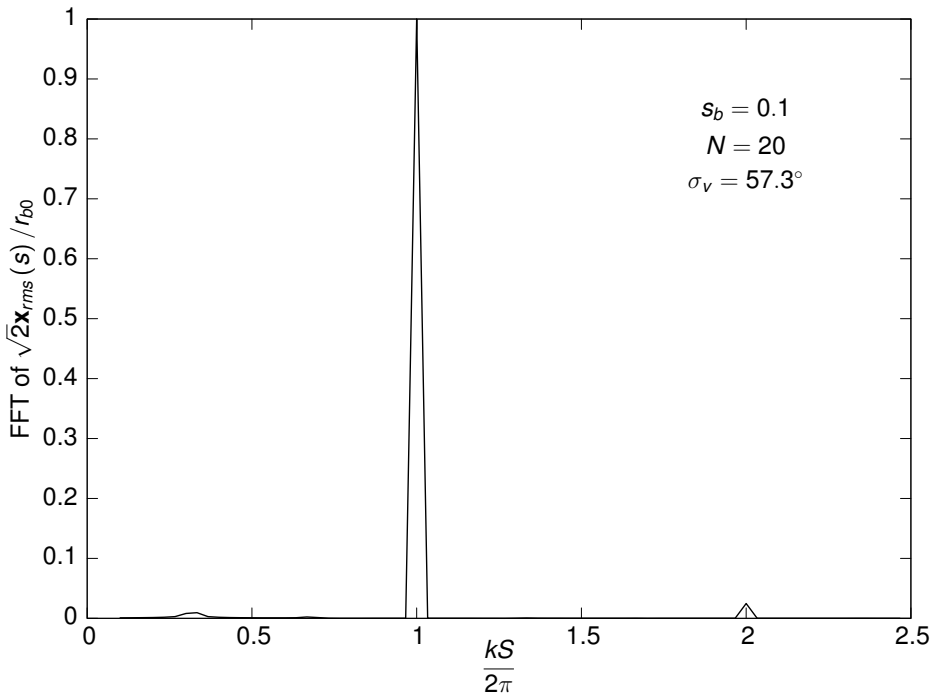

Figure: FFT of $\sqrt{2}x_{rms}(s)/r_{b0}$ for $N = 20$. The left figure is FFT from $s = 0$ to $s = 30S$, and the right figure is FFT from $s = 270S$ to $s = 300S$.

Solution of the Envelope Equation

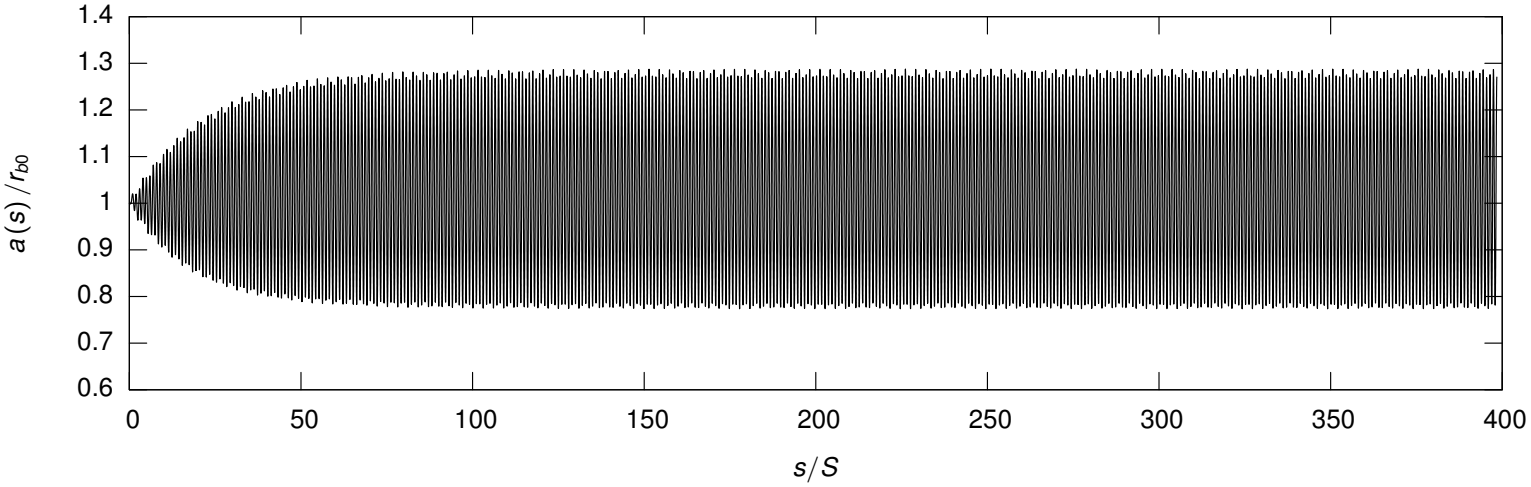

Figure: Time evolution in the **x** direction for $N = 20$ (slow turn-on). In the figure, x_{rms} is the root mean square x for all the particles.

For beam with $s_b = 0.1$, the δf simulation of the Vlasov-Maxwell equation agrees quite well with the simulation of the envelope equation for the same adiabatic turning-on model.

Solution of the Envelope Equation

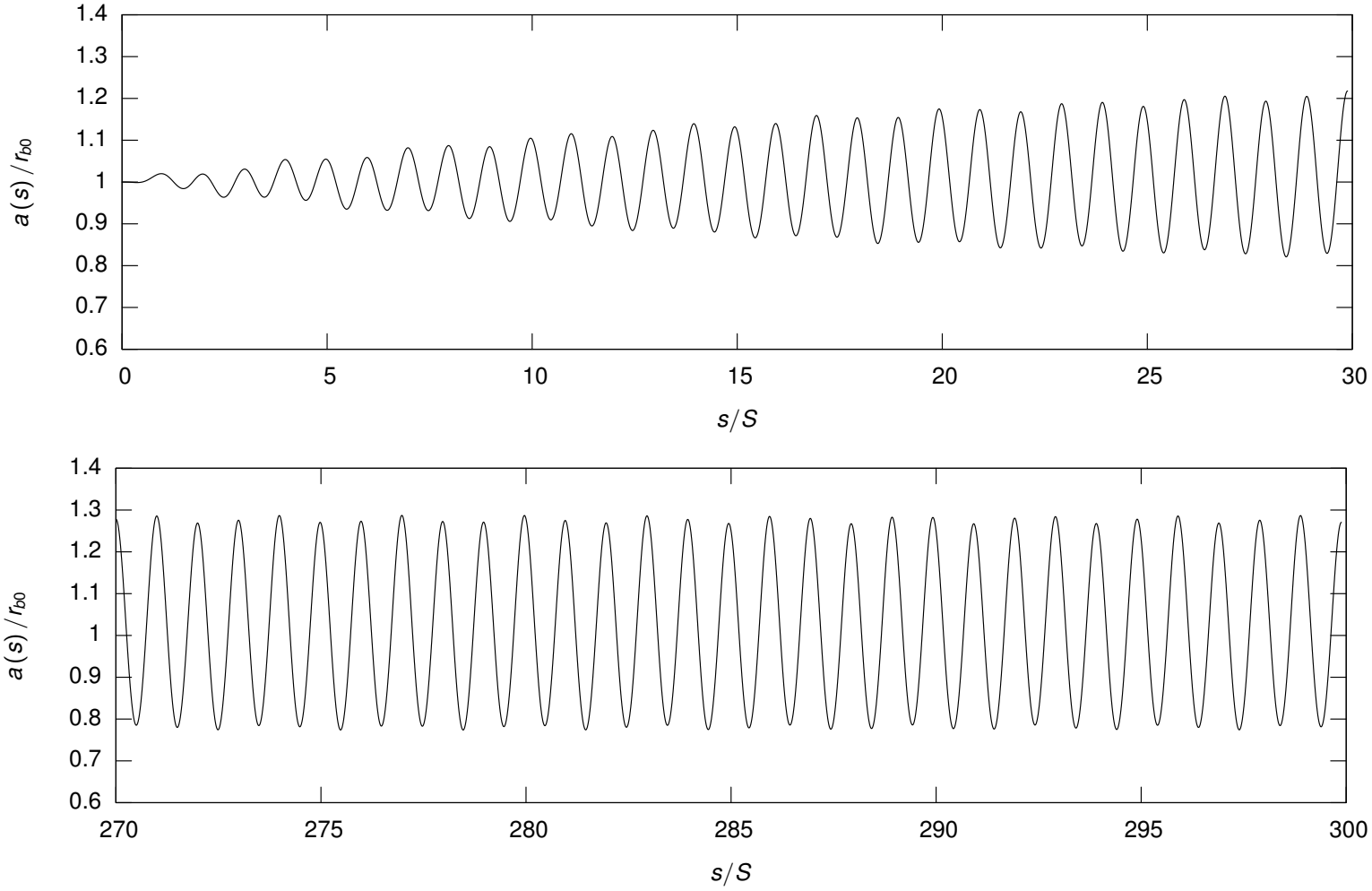

Figure: Time evolution in the **x** direction for $N = 20$ (slow turn-on)

Conclusion and Future Plan

- For the solenoidal lattice configuration:
  - By adiabatically replacing the smooth-focusing lattice with the periodic solenoidal lattice in the δf simulation, we can obtain good matched beam after sufficient time.
  - With the slower turn-on model, we can obtain better beam matching than the faster turn-on model.
  - The beam with higher intensity matches the solenoidal lattice better than the beam with lower intensity.

- For the quadrupole lattice configuration:
  When the normalized intensity $s_b = 0.1$, δf simulation of the Vlasov-Maxwell equation agrees with the simulation of the envelope equations. Similar to the solenoidal case, we can obtain rather good matched beam after sufficient time. Actually when s_b is small enough ($s_b < 0.7$), we can always obtain good matched beam after sufficient time.

- More simulations for the quadrupole lattice configuration will be carried out to investigate the dynamics of the quadrupole focused beam.